Nuclear Engineering and Technology 52 (2020) 1036–1042

Contents lists available at ScienceDirect

Nuclear Engineering and Technology

journal homepage: www.elsevier.com/locate/net

Original Article

# A $^{235}$U mass measurement method for $UO_2$ rod assembly based on the n/γ joint measurement system

Jianqing Yang [a, b, 1], Quanhu Zhang [a, *, 1], Xianghua Su [a, 1], Sufen Li [a, 1], Lin Zhuang [a], Suxia Hou [a], Yonggang Huo [a], Hao Zhou [c], Guorong Liu [c]

[a] Xi'an Research Institute of Hi-Tech, 710025, Xi'an, China
[b] Institute of High Energy Physics, Chinese Academy of Sciences, Beijing, 100049, China
[c] China Institute of Atomic Energy, 102413, Beijing, China

ARTICLE INFO

*Article history:*
Received 8 July 2019
Received in revised form
28 September 2019
Accepted 22 October 2019
Available online 23 October 2019

*Keywords:*
Fast-neutron multiplicity counter
n/γ joint measurement system
Liquid scintillator detector
HPGe γ spectrometer
$UO_2$ rod assembly
$^{235}$U mass

ABSTRACT

Fast-Neutron Multiplicity Counter based on Liquid Scintillator Detector can directly measure the fast neutron multiplicity emitted by $UO_2$ rod. HPGe gamma spectrometer; which has superior energy resolution; is routinely used for the gamma energy spectrum measurement. Combing Fast-Neutron Multiplicity Counter and HPGe γ-spectrometer, the n/γ joint measurement system is developed. The fast neutron multiplicity and gamma energy spectrum of $UO_2$ rod assemblies under different conditions are measured by the n/γ joint measurement system. The induced fission rate and the $^{235}$U abundance, thereby the $^{235}$U mass; can be obtained for $UO_2$ rod assemblies. The $^{235}$U mass deviation of the measured value from the reference value is less than 5%. The results show that the n/γ joint measurement system is effective and applicable in the measurement of the $^{235}$U mass in samples.


## 1. Introduction

The $^{235}$U mass properties measurement of special nuclear materials in sealed containers has always been an important issue in the fields of nuclear security, nuclear non-proliferation and military control verification [1]. In the traditional detection, the joint measurement system including HPGe gamma spectrometer and $^{3}$He detector is used to detect and characterise neutrons and gamma rays directly emitted from nuclear materials [2]. An array of moderated pressurized $^{3}$He detectors was utilized to determine singles, doubles, triples and more coincidences in Neutron multiplicity measurements [3]. $^{3}$He detector has a higher detection efficiency. However, $^{3}$He detector can only measure moderated neutrons which will lose some information and is very expensive because of dozens of $^{3}$He tubes. Compared with $^{3}$He detector, Liquid Scintillation Detector is more economical, has a good n/γ discrimination capability as well as can measure fast neutrons directly and record more information which has attracted a lot of attention [4,5]. At the same time, although the detection efficiency of Liquid Scintillation Detector is not higher than that of $^{3}$He detector, it is still enough for the measurement of $^{235}$U mass. Thus, the joint measurement system including HPGe gamma spectrometer and Liquid Scintillation Detector has some advantages whether it is in information acquisition or price.

In recent years, A. Pozzi of the University of Michigan and others have conducted in-depth research on fast neutron multiplicity measurement methods and techniques based on Liquid Scintillation Detectors, and built a detection system based on EJ-309 detector [6]. The equivalent mass of metal samples was measured and analyzed based on this detection system [7]. M. Verbeke et al. of the Lawrence Livermore National Laboratory measured and analyzed the neutron multiplicity and the emitted neutron energy spectrum of Pu and $PuO_2$ samples [8]. In the meantime, Gamma spectroscopy is a nondestructive technique that measures the energy spectrum of gamma rays naturally emitted from U material. HPGe detector presents an excellent solution in screening commercial and personal vehicles, aerial and ground radiation surveys, stand-off detection, and gamma-ray imaging [9].

In a previous work by the authors, a fast neutron multiplicity

* Corresponding
*E-mail addresses:* yangjianqing@ihep.ac.cn (J. Yang), zhangqh_102@sina.com (Q. Zhang).
[1] These authors contributed equally.

https://doi.org/10.1016/j.net.2019.10.018

measurement equation was established based on theoretical analysis and the validity was verified based on the simulation studies [10,11], At the same time, Liquid Scintillator Detector of six probes was built, the samples were preliminary measured and analyzed and ideal results were obtained based on this device [12].

Based on the previous theoretical approach, computer simulation and preliminary experimental research, we build the n/γ joint measurement system containing HPGe gamma spectrometer, Liquid Scintillator Detector of six probes, an external AmLi neutron source together with electronics and data processing system. As such, Fast-Neutron Multiplicity Counter; based on Liquid Scintillator Detector; can directly measure the fast neutrons emitted by $UO_2$ rod and the induced fission rate can be determined. HPGe gamma spectrometer is used for the gamma energy spectrum measurement and $^{235}U$ abundance in $UO_2$ rod can be obtained. Combining Fast-Neutron Multiplicity Counter and HPGe gamma spectrometer, we can get the induced fission rate and the $^{235}U$ abundance of $UO_2$ rod, thereby the $^{235}U$ mass.

In this experiment, the fast neutron multiplicity and gamma energy spectrum of $UO_2$ rod assemblies with different abundances, different masses and in different positions are measured and analyzed by the n/γ joint measurement system. the neutrons and γ rays emitted from samples are measured, fast neutron multiplicity, $^{235}U$ abundance and $^{235}U$ mass of samples are obtained. The relative deviation of $^{235}U$ mass measurement is less than 5% which shows that the n/γ joint measurement system is effective and applicable in the measurement of $^{235}U$ mass in samples. The results provide related technical support for nuclear security, nuclear non-proliferation and military control verification.

## 2. Fast neutron multiplicity counter and measurement method

### 2.1. The n/γ joint measurement system

In order to obtain the total mass of U samples, it is necessary to measure the induced fission rate $F$ and abundance of $^{235}U$. The measurement device is a self-developed n/γ joint measurement system. The system consists of two parts: one is Fast-neutron Multiplicity Counter, the other is HPGe gamma energy spectrum measurement system. The schematic diagram of the n/γ joint measurement system is shown in Fig. 1.

### 2.2. The n/γ joint measurement method

The n/γ joint measurement system mainly includes the fast neutron multiplicity measurement which is performed by Fast-Neutron Multiplicity Counter and the gamma energy spectrum measurement which is performed by HPGe gamma spectrometer. In the previous work, we established the high order fast neutron multiplicity measurement equation including singlets, doublets, triplets, quadruplets and pentuplets and a mathematical model to symbolize the detection processes of fission neutrons which lay a theoretical and analytical foundation for the research [10–13]. The induced fission rate and abundance of U samples can be obtained and thereby the $^{235}U$ mass properties can be determined. The schematic diagram of the U sample measurement principle is shown in Fig. 2.

Where $M$ is the proliferation coefficient, $P$ is the number distribution matrix of neutrons emitted from samples, $Q$ is the detection efficiency matrix, $T$ is the signal recording matrix, and $R$ is the signal multiplicity matrix.

$$M = \frac{1-q}{1-q\cdot\nu} \tag{1}$$

where q is the average probability of secondary fission caused by primary fission neutrons, $\nu$ is the average number of fission neutrons of the second fission event. In this work, $\nu$ is set to 2.64 for $^{235}U$.

#### 2.2.1. Fast neutron multiplicity analysis of the U fission rate

Since the spontaneous fission rate of $^{235}U$ is low, an external neutron source is required to induce fission. As such, many neutrons will be generated through a self-proliferation process in the sample. These neutrons are detected and recorded by Fast-Neutron Multiplicity Counter. Singlet, Doublet, Triplet, Quadruplet, Pentuplet and Sextuplet of neutrons can be gotten by analyzing the data using the developed program [10]. The fast neutron generation and detection process is shown in Fig. 2.

Based on studying the induced fission neutron production and self-proliferation of U samples and detection processes, a measurement matrix analysis equation of U fast neutron multiplicity is established by using the factorial moments and parameter estimation two analytical methods. This equation describes the relationship between the measurement parameters (i.e., the count rates: $R_1$、$R_2$、$R_3$ and $R_4$) and the sample parameters (the induced fission rate, self-proliferation coefficient and detection efficiency). By solving the equation, the property parameters of the sample can

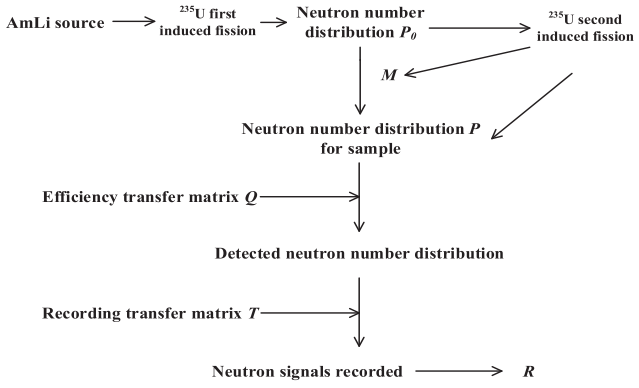


**Fig. 2.** U sample measurement principle.

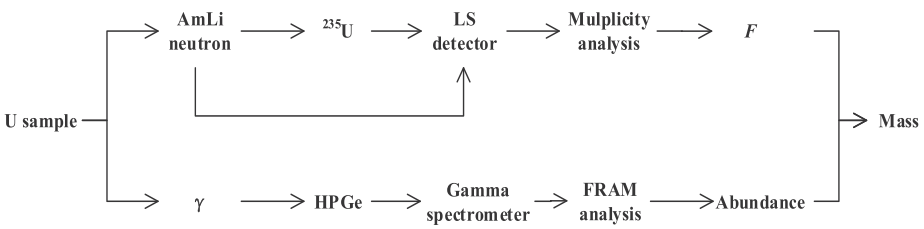


**Fig. 1.** The schematic diagram of the n/γ joint measurement system.

be obtained.

According to reference [12], the measurement matrix analysis equation of fast neutron multiplicity can be obtained, as shown in equation (2).

$$R_{1\times6} = FP_{1\times14}(q)Q_{14\times14}(\varepsilon)T_{14\times6} \tag{2}$$

where $F$ is the induced fission rate, $\varepsilon$ is the detection efficiency of the detection system. The measured data includes the total number of neutrons $C_1$,$C_2$,$C_3$,$C_4$,$C_5$ and $C_6$ recorded by each detector. $R_1$, $R_2$, $R_3$, $R_4$, $R_5$ and $R_6$ represents Singlet, Doublet, Triplet, Quadruplet, Pentuplet and Sextuplet counting rates respectively. The number of detected neutrons is used for $P$ matrix calculation after subtracting the AmLi source background.

The unknowns contained in Equation (2) are $F$, $q$ and $\varepsilon$. In the actual measurement process, $R_1$ is easily affected by background radiation which results in deviation from the real values. The counting rates $R_5$ and $R_6$ are extremely low. When this measurement system works for 20 h, $R_5$ and $R_6$ are still close to zero. Therefore $R_2$, $R_3$, and $R_4$ are used to solve equation (2) which can be transformed into equation (3).

$$\begin{cases} f_1(q,\varepsilon) = 0 \\ f_2(q,\varepsilon) = 0 \end{cases} \tag{3}$$

It is difficult to solve equation (3) directly, and it is transformed into the equivalent equation No. (4).

$$f = f_1^2 + f_2^2 \tag{4}$$

where $f = 0$ is the goal of solving the equation, the iterative method is used to solve equation (4), and $q$ and $\varepsilon$ can be obtained under the condition that $f$ is close enough to 0. The induced fission rate $F$ can be obtained after substituting $q$ and $\varepsilon$ into equation (2). The self-proliferation coefficient $M$ can be obtained after bringing $q$ into equation (1). The details about how to solve equation (4) can be known in part 3.2 of reference [13].

In order to obtain the mass of $^{235}$U, we propose the following calculation method. First, the equivalent coefficient $C_{eff}$ is defined, which means that the total number of induced fission neutrons contributed by the unit mass $^{238}$U is equivalent to the total number of fission neutrons contributed by $^{235}$U whose mass is $C_{eff}$. Therefore, the equivalent mass of the sample can be expressed as equation (5).

$$m_{eff} = m_{235} + C_{eff} \cdot m_{238} \tag{5}$$

where $m_{eff}$ represents the equivalent $^{235}$U mass of the sample, and $m_{235}$ and $m_{238}$ represents the mass of $^{235}$U and $^{238}$U in the sample respectively. Thereby, the relationship between the induced fission rate $F$ and the equivalent mass can be obtained which is shown in equation (6).

$$F = F(m) \tag{6}$$

Through many measurements, we make some calibrations according to the known sample properties. The empirical formula (6) and the equivalent coefficient $C_{eff}$ are obtained. And the expression of solving $^{235}$U mass through the fission rate can be obtained according to the calibration relationship.

#### 2.2.2. Gamma spectrum analysis of the U abundance

The U sample contains $^{235}$U and $^{238}$U isotopes. By measuring the $\gamma$ energy spectrum of the isotope and analyzing the relationship between the full energy peak count and the nuclide activity, the branching ratio and the detection efficiency of the full energy peak, the isotope abundance of the U sample can be obtained [14].

There are two kinds of isotopic abundance analysis methods and corresponding software which are commonly used. One is MGA which is developed by Lawrence Livermore National Laboratory and used to analyze the plutonium isotopic abundance. It can detect the$\gamma$rays, whose energy is between 94 and 104 kev, emitted from plutonium materials [15]. Another is FRAM which is developed by Los Alamos National Laboratory and used to analyze the uranium and plutonium isotopic abundance [16]. It can detect the$\gamma$rays, whose energy is between 140 and 1001kev, emitted from uranium and plutonium materials.

In this work, the uranium isotopic abundance is measured by the FRAM method. The FRAM method is relatively simple and the requirements for the resolution and stability of the detector are relatively loose. The efficiency is corrected by the efficiency approximation or the relative efficiency self-calibration technique, thereby the activity ratio of $^{235}$U and $^{238}$U is calculated and the isotopic abundance of U is obtained.

According to the principle of the FRAM method, the relative efficiency curve function definition is expressed as equation (7).

$$f(E) = \ln(AE) = \ln\left(\frac{n}{BR}\right) \tag{7}$$

where $n$ is the net counting rate of the full energy peak, $BR$ is the branching ratio, $A$ is the nuclide activity, and $\varepsilon$ is the full energy peak efficiency. For each energy peak from the same nuclide, the corresponding activity is the same. A relative efficiency curve can be given for each of multiple characteristic peaks of $^{235}$U and $^{238}$U.

$$f_{235}(E) = \ln(A_{235}\varepsilon) = \ln\left(\frac{n_{235}}{BR_{235}}\right) \tag{8}$$

$$f_{238}(E) = \ln(A_{238}\varepsilon) = \ln\left(\frac{n_{238}}{BR_{238}}\right) \tag{9}$$

Assuming $A_{235} = kA_{238}$, where $k$ is a coefficient, formula (10) can be obtained as follows:

$$f_{235}(E) = \ln(kA_{235}\varepsilon) = f_{238}(E) + \ln k \tag{10}$$

Therefore, the two curves have the same shape with a fixed difference between them. The difference is determined by abundance. The best $k$ value can be determined by making the two curves coincide using curve fitting, and the isotopic abundance of U sample can be calculated.

In this work, the $^{235}$U characteristic $\gamma$-rays with an energy of 185.72 MeV (branch ratio 57.0%) are selected, but $^{238}$U characteristic $\gamma$ rays cannot be observed. Because the characteristic $\gamma$ rays of $^{235}$U is in the medium energy range which can be detected and analyzed effectively. However, the characteristic $\gamma$ rays of $^{235}$U is mostly in the high energy range which haven't overlapping area with the medium energy range. Thus we select the characteristic $\gamma$-rays, whose energy is 1001.03 keV (branche ratio 0.842%), of the decaying body $^{234}$Pa of $^{238}$U.

## 3. Experimental study on mass measurement of $UO_2$ rod assembly

### 3.1. The n/$\gamma$ joint measurement system experimental device

The n/$\gamma$ joint measurement system includes Fast-Neutron Multiplicity Counter and HPGe gamma spectrometer. Fast-Neutron Multiplicity Counter mainly includes BC501A detector, external AmLi neutron source, sample room, MPD-4 four-channel pulse shape discriminator, MCA-6A multichannel time analyzer

and data processing analysis software, etc. HPGe gamma spectrometer mainly includes HPGe gamma detector, Inspector-2000 multichannel gamma spectrometer and energy spectrum analysis software. The main components of Fast-Neutron Multiplicity Counter and HPGe gamma spectrometer are shown in Tables 1 and 2.

The Liquid Scintillation Detector used in this work is an BC501A, and the active area is a cylinder 3 inches thick and a diameter of 5 inches. The BC501A detector has a dead time of 64 ns, and the detection threshold is set to about 120 keV, and the counting coincidence gate width is set to 100 ns? There are six BC501A detectors around the sample room. The detector system is shown in Fig. 3.

The MPD-4 is mainly used for n/γ discrimination. According to the different output characteristics of the two kinds of signals, we can adjust the parameters by the computer serial port control so that the system can achieve the required discrimination effect. The MCS-6A is a multichannel time analyzer with 100 ps resolution and is mainly used in time-of-flight measurement and position sensitive detection systems. The neutron time-of-flight information recorded by the MCS-6A can be transmitted to a computer and stored in a data file in the form of LIST-mode [17], and then the data is processed by the root software.

### 3.2. Detection efficiency and background measurement

A$^{252}$Cf source with an activity of 4.44 × 105Bq is used in the detection efficiency calibration measurement. During the experiment, the $^{252}$Cf source is placed in different positions of the effective space region, and the detection efficiency is measured. The experimental results show that the detection efficiency in the center of the effective space region is 7%. Taking the detection efficiency in the center of the effective space region as a reference, the detection efficiencies in different positions of the horizontal and vertical direction are shown in Fig. 4 and Fig. 5 respectively.

It can be seen from Figs. 4 and 5 that the system is symmetrical. The experimental measurement results show that the maximum detection efficiency deviation is less than 1.5% in 6 × 6 × 8 cm$^3$ sample cavity in the center of the effective space region. Thus, this experimental system satisfies the uniformity requirement of detection efficiency [Reference].

During the background measurement experiment, only the AmLi source is placed and measured using a fast neutron multiplicity system. The experiment is divided into three groups each counted for 3600s each. The measured channel counts are shown in Table 3. Based on the relative relationship of the average counts, the relative detection efficiency of the probes can be obtained.

By processing the data above, Singlets, Doublets, Triplets and Quadruplets are obtained by the three measurements which are shown in Table 4.

It can be seen from Table 4 that the difference among the different groups is large for Triplets and Quadruplets, because they mainly come from the background radiation, rather than the accidental conficidence of the neutrons emitted by the AmLi source.

**Table 1**
Fast neutron multiplicity counter system.

| Name | Model | Quantity |
|---|---|---|
| Liquid Scintillator Detector | BC501A | 6 |
| n/γ pulse waveform discriminator | MPD-4 | 2 |
| Multichannel time measurement instrument | MCS6a | 1 |
| Digital multichannel counter | MCA-8000 | 1 |
| External neutron source | AmLi source | 2 |

**Table 2**
HPGe γ spectrometer.

| Name | Model | Quantity |
|---|---|---|
| Gamma detector | HPGe | 1 |
| Multichannel spectrometer | Inspector-2000 | 1 |

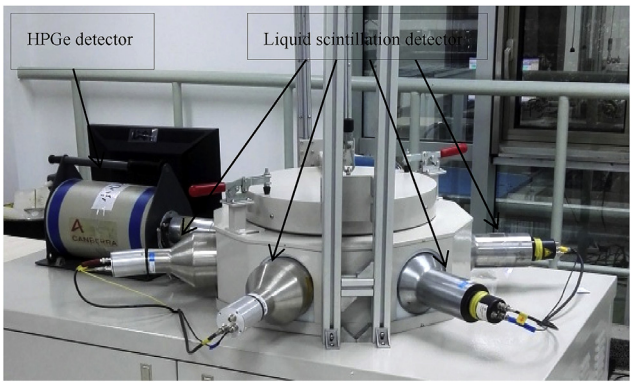


**Fig. 3.** The n/γ joint measurement system.

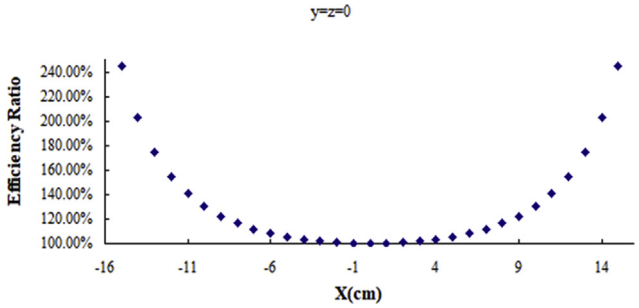


**Fig. 4.** Detection efficiency ratio in different positions in the horizontal direction.

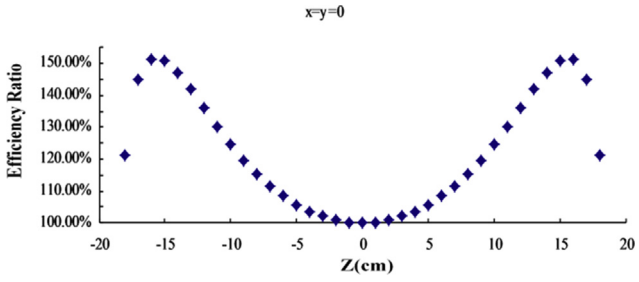


**Fig. 5.** Detection efficiency ratio in different positions in the vertical direction.

### 3.3. Abundance measurement

The $UO_2$ rod assembly used in the experiment consists of $UO_2$ rods with 4.2% and 10% abundances. Using HPGe gamma spectrometer, the gamma energy spectrum is measured and the data is stored in the ".TKA" file in ASCII format. The ROOT software was used to process and analyze the data directly. The actual measured energy spectrum is shown in Fig. 6.

The peak in the total count can be found by program and then the corresponding channel AmLi count is subtracted from the total

**Table 3**
AmLi source measurement channel count.

| Number of groups | 1 | 2 | 3 | Average value | Relative detection efficiency |
|---|---|---|---|---|---|
| Channel 1 | 148858 | 148490 | 148517 | 148622 | 0.168852 |
| Channel 2 | 159019 | 158880 | 158837 | 158912 | 0.180543 |
| Channel 3 | 127439 | 127844 | 127658 | 127647 | 0.145022 |
| Channel 4 | 136026 | 135810 | 135989 | 135942 | 0.154446 |
| Channel 5 | 139204 | 138574 | 138076 | 138618 | 0.157487 |
| Channel 6 | 168985 | 170752 | 171606 | 170448 | 0.193649 |

**Table 4**
AmLi source count rate.

| Counting rate | 1 | 2 | 3 | Average value |
|---|---|---|---|---|
| Singlets | 243.6956 | 243.9500 | 244.0678 | 243.9045 |
| Doublets | 0.290793 | 0.278295 | 0.281389 | 0.283492 |
| Triplets | 0.000554 | 0.000378 | 0.001101 | 0.000678 |
| Quadruplets | 0.000278 | 0.000132 | 0.000008 | 0.000139 |

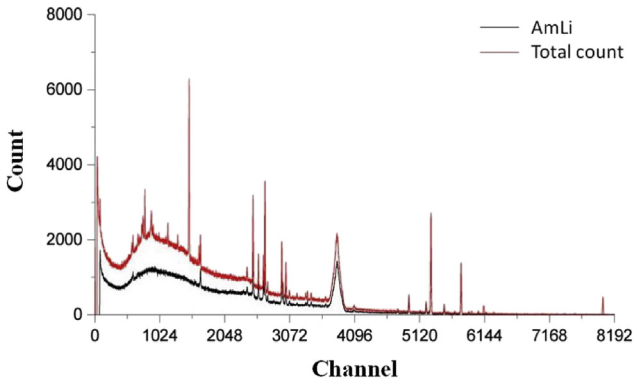


**Fig. 6.** Measurement of U and AmLi γ energy spectrum.

peak count and the relative efficiency curves are fit. Several groups of $UO_2$ rod assemblies are measured and calculated, and the abundance measured values and relative-deviation values are obtained as shown in Table 5.

As can be seen from Table 5, the relative deviation of measured abundance for $UO_2$ rod assembly is basically less than 10%, and the measurement deviation becomes larger with the increase of $UO_2$ rod assembly number and abundance. When $UO_2$ rod assembly number increases, the measured abundance decreases gradually. This is mainly due to the cascade decay relationship among characteristic gamma rays of $^{234}$Pa. Meanwhile, the position of the bracket hole which fixes $UO_2$ rod leads to the mutual occlusion between the samples, which has the same effect as reducing the stereoscopic angle of the detector. The coincidence addition effect is weakened, and the characteristic γ-rays count of 1001.03 keV is relatively reduced. As a result, the $^{238}$U abundance will increase and the $^{235}$U abundance will decrease when we analyze the data.

### 3.4. $^{235}$U mass measurement for $UO_2$ rod assembly

The U sample used in the experiment is a $UO_2$ rod composed of $^{235}$U and $^{238}$U isotopes. The $^{235}$U in $UO_2$ rods has 4.2% and 10% two abundances, and the parameters of each U sample with different abundances are shown in Table 6.

In the experiment, the actual measurement object is a $UO_2$ rod assembly composed of multiple $UO_2$ rod. The measurement object is placed in the mesh plate which has 64 (8 × 8) meshes as shown in Fig. 7. Considering the uniformity of space detection efficiency and the experimental conclusion of detection efficiency, only 16 (4 × 4) meshes in the middle are used to place samples, which are the effective area of the detection space. The size of the effective area is 6 cm × 6 cm.

The experiment is divided into three cases.

In the first case, $UO_2$ rods with 4.2% abundance are used, the experiment is divided into three groups. In the first, second and third group, the measured sample consists of 8, 12 and 16 $UO_2$ rods respectively.

In the second case, $UO_2$ rods with 10% abundance are used. Like the first case, the experiment is divided into three groups. In the first, second and third groups, the numbers of the experimental $UO_2$ rods numbers are 3, 5, and 8 respectively.

In the third case, $UO_2$ rods with two abundances are used. In the first group of experiments, the measured sample consists of 2 $UO_2$ rods with 4.2% abundance and 2 $UO_2$ rods with 10% abundance. In the second group, the measured sample consists of 3 $UO_2$ rods with 4.2% abundance and 3 $UO_2$ rods with 10% abundance. In the third

**Table 6**
Uranium sample parameters.

| Abundance (%) | Uranium total quantity per rod (g) | $^{235}$U quantity per rod (g) |
|---|---|---|
| 4.2 | 37.23 | 1.56 |
| 10 | 38.19 | 3.82 |

**Table 5**
U sample abundance measurement results.

| Number of UO2 rods | Reference Abundance (%) | Measured Abundance (%) | Relative deviation (%) | Reference Abundance (%) | Measured Abundance (%) | Relative deviation (%) |
|---|---|---|---|---|---|---|
| 8 | 4.2 | 4.37 | 0.041 | 10 | 10.26 | 0.061 |
| 9 | 4.2 | 4.28 | 0.020 | 10 | 10.02 | 0.003 |
| 10 | 4.2 | 4.27 | 0.016 | 10 | 9.84 | −0.039 |
| 11 | 4.2 | 4.14 | −0.015 | 10 | 9.89 | −0.026 |
| 12 | 4.2 | 4.15 | −0.011 | 10 | 9.85 | −0.036 |
| 13 | 4.2 | 4.15 | −0.012 | 10 | 9.78 | −0.053 |
| 14 | 4.2 | 4.12 | −0.020 | 10 | 9.66 | −0.080 |
| 15 | 4.2 | 4.11 | −0.020 | 10 | 9.55 | −0.107 |
| 16 | 4.2 | 4.06 | −0.033 | 10 | 9.42 | −0.139 |

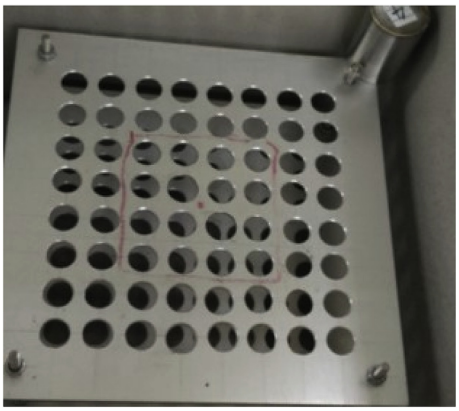

**Fig. 7.** Sample placement mesh plate.

group, the measured sample consists of 4 $UO_2$ rods with 4.2% abundance and 4 $UO_2$ rods with 10% abundance.

Because the activity of the sample is low and the measured $R_4$ is small, the actual measured parameters are the counting rates $R_1$, $R_2$ and $R_3$. The parameters of the different cases are shown in Table 7.

According to the experimental measurements $R_1$, $R_2$ and $R_3$, the induced fission rates of different cases are solved by equation (11).

According to the relationship between the induced fission rate $F$ and equivalent $^{235}U$ mass, the empirical formula (11) is obtained.

$$F = 53.88 + 25.67m - 0.1m^2 \tag{11}$$

The equivalent coefficient $C_{eff}$ in this work is 0.043. According to the equations and parameters obtained through the calibration, the $^{235}U$ mass under different experimental conditions can be obtained, and the relative deviation between the measured value and the reference value can be obtained. The result illustrates that the relative deviation is less than 5% which is shown in Table 8.

In order to study the influence of different positions of the same measurement object on the experimental results in the effective space region. The measurement object is set to 8 $UO_2$ rods with 10% abundance and placed in different positions which is shown in Fig. 8. The effects of different measurement positions on induced fission rate are studied. The measurement and calculation results are shown in Table 9.

Measurement and calculation results are shown in Table 9, Where $R_1$, $R_1$, and $R_1$ are singlets, doublets and triplets, and $F$ is the induced fission rate. Through the above measurement and analysis results, it is found that the induced fission rate deviation is within 3% and the $^{235}U$ mass deviation is less than 5% when the same sample is placed in different positions. Thereby, it shows that the space detection efficiency uniformity is good in the effective spatial

**Table 7**
Parameter value of different cases.

| Experimental cases | Experimental grouping | $UO_2$ rods number (4.2% abundance) | $UO_2$ rods number (10% abundance) | $R_1$ | $R_2$ | $R_3$ | $F$ |
|---|---|---|---|---|---|---|---|
| First | First group | 8 | | 612369 | 9143 | 252 | 636.85 |
| | Second Group | 12 | | 673950 | 12376 | 309 | 872.89 |
| | Third group | 16 | | 732022 | 15275 | 354 | 1098.19 |
| Second | First group | | 3 | 560971 | 6653 | 183 | 448.63 |
| | Second Group | | 5 | 622056 | 9969 | 259 | 677.24 |
| | Third group | | 8 | 682650 | 13103 | 329 | 904.54 |
| Third | First group | 2 | 2 | 559412 | 6541 | 177 | 429.6 |
| | Second Group | 3 | 3 | 609396 | 9127 | 235 | 631.09 |
| | Third group | 4 | 4 | 656661 | 11703 | 344 | 814 |

**Table 8**
Comparison of reference value and measured value.

| Cases | Groups | Number of $UO_2$ rod (4.2%) | Number of $UO_2$ rods (10%) | $^{235}U$ mass Reference values (g) | $^{235}U$ mass Measurement values (g) | Relative deviation (%) |
|---|---|---|---|---|---|---|
| First | First group | 8 | | 12.48 | 12.58 | 0.78% |
| | Second group | 12 | | 18.72 | 18.7 | −0.11% |
| | third group | 16 | | 24.96 | 24.22 | −2.99% |
| Second | First group | | 3 | 11.46 | 11.75 | 2.55% |
| | Second Group | | 5 | 19.1 | 19.56 | 2.42% |
| | Third group | | 8 | 30.56 | 31.15 | 1.92% |
| Third | First group | 2 | 2 | 10.76 | 11.22 | 4.3% |
| | Second group | 3 | 3 | 16.14 | 16.7 | 3.5% |
| | Third group | 4 | 4 | 21.52 | 21.3 | −1% |

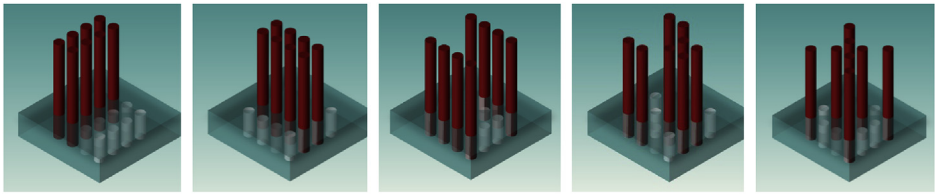

A B C D E

**Fig. 8.** Sample placement configuration.

**Table 9**
Measurement and calculation results.

| Configuration | Measured value | | | Calculated value | | |
|---|---|---|---|---|---|---|
| | $R_1$ | $R_2$ | $R_3$ | $F$ | $^{235}$U mass (g) | Relative deviation (%) |
| A | 692310 | 13841 | 374 | 967.85 | 30.79 | 0.74 |
| B | 696715 | 14094 | 398 | 958.65 | 30.50 | −0.21 |
| C | 710081 | 14837 | 388 | 1008.2 | 32.07 | 4.94 |
| D | 707069 | 14753 | 385 | 991.07 | 31.53 | 3.16 |
| E | 708882 | 14879 | 358 | 997.46 | 31.73 | 3.82 |

range, and the influence of the sample distribution; in the detection space; on the result is negligible.

## 4. Conclusion and discussion

In this work, we developed the n/γ joint measurement system. Fast neutron multiplicity and the abundance are measured for multiple groups of $UO_2$ rod assemblies under different conditions. By using the fast neutron multiplicity matrix analysis equation and the relationship between the induced fission rate and the equivalent mass, the mass of the $UO_2$ rod assembly is obtained, and the deviation between the measured value and reference value is less than 5%.

For the neutron multiplicity measurement and the mass analysis of the U-material in the sealed container, it is also necessary to consider the effect of the container-packaging on the resulting measurement and how to get the quantitative relationship between the induced fission rate and the equivalent mass. This problem will be further considered in depth in future work.

## Declaration of competing interests

We declare that we have no financial and personal relationships with other people or organizations that can inappropriately influence our work, there is no professional or other personal interest of any nature or kind in any product, service and/or company that could be construed as influencing the position presented in, or the review of, the manuscript entitled.

## Acknowledgments

The authors extend their sincere thanks to The National Nature Science Fund of China Grants; Agreement Number 51309228; for the financial support for this work. The project is also funded by China Postdoctoral Science Foundation (No. 2013M542459). The authors are also thankful to the Shaanxi Technology Committee; Natural Science Basic Research Project No. 2016JM6026; for the financial support.

The authors completed the work of this paper with the cooperation of CIAE researchers and received enthusiastic help so that the work can be completed better and faster. As such, the authors are highly grateful for this.

## References

[1] D.G. Langner, J.E. Stewart, M.M. Pickrell, et al., Application Guide to Neutron Multiplicity Counting, Office of Scientific & Technical Information Technical Reports, 1998 (1998) Los Alamos Report LA-13422-M.
[2] Hajir Al Hamrashdi, Stephen D. Monk, David Cheneler, Passive gamma-ray and neutron imaging systems for National security and nuclear non-proliferation in controlled and uncontrolled detection areas: review of past and current status, Sensors 19 (2019) 2638.
[3] R.T. Kouzes, B.D. Geelhood, Methods for Attribute Measurement and Alternatives to Multiplicity Counting, 2000. PNNL-13250.
[4] M. Flaska, S.A. Pozzi, Identification of shielded neutron sources with the liquid scintillator BC-501A using a digital pulse shape discrimination method, Nucl. Instrum. Methods Phys. Res. Sect. A Accel. Spectrom. Detect. Assoc. Equip. 577 (3) (2007) 654–663.
[5] L.F. Nakae, G.F. Chapline, A.M. Glenn, et al., The use of fast neutron detection for materials accountability, Int. J. Mod. Phys. Conf. Ser. 27 (2014) 1460140.
[6] S.A. Pozzi, M.C. Hamel, J.K. Polack, et al., Detection for nuclear Nonproliferation, in: Proceedings of International Symposium on Radiation Detectors and Their Uses (ISRD2016), 2016, 050001, 5.
[7] J.R. Wachter, E.L. Adams, N. Ensslin, Prototype fast neutron counter for the assay of impure plutonium, Trans. Am. Nucl. Soc. 55 (1987). LA-UR-87-3678.
[8] J.M. Verbeke, G.F. Chapline, S.A. Sheets, Distinguishing Pu metal from Pu oxide and determining α-ratio using fast neutron counting[J], Nucl. Instrum. Methods Phys. Res. A782 (2015) 126–132.
[9] S. Stave, Germanium Detectors in Homeland Security at PNNLJournal of Physics: Conference Series, IOP Publishing, 2015, 012018, 606(1).
[10] Sufen Li, Suizheng Qiu, Quanhu Zhang, et al., Fast-neutron multiplicity analysis based on scintillation, Appl. Radiat. Isot. 110 (2016) 53–58.
[11] Q. Zhang, S. Li, L. Zhuang, et al., Simulation study on neutron multiplicity of plutonium based on liquid scintillation detector, Appl. Radiat. Isot. 135 (2018) 92–98.
[12] Hao Zhou, Hongtao Lin, Guorong Liu, et al., A neutron multiplicity analysis method for uranium samples with liquid scintillators, Nucl. Instrum. Methods Phys. Res. 797 (2015) 70–76.
[13] Quanhu Zhang, JianqingYang XinsheLi, et al., High order fast neutron multiplicity measurement equations based on liquid scintillation detector, Appl. Radiat. Isot. 152 (2019) 45–51.
[14] Peijia Tang, Kunpen Li, Determination of isotopic abundance of uranium and plutonium by γ-ray spectrometry, J. Isot. (Z1) (2001) 166–173.
[15] T.A. Kelley, PC/FRAM: Algorithms for the Gamma-Ray Spectrometry Measurement of Plutonium Isotopic Composition, LA-UR-95–3326, USA, 1995, pp. 3–5.
[16] R. Gunnink, MGA: A Gamma-Ray Spectrum Analysis Code for Determining Plutonium Isotopic Abundances UCRL-LR-103220,USA, 1990, pp. 2–3.
[17] I. Israelashvili, Janos Bagi, J. Huszti, LIST-mode applications for neutron multiplicity counting, Nucl. Instrum. Methods Phys. Res. 735 (2014) 53–59.